

Tree carbon allocation dynamics determined using a carbon mass balance approach

Tamir Klein and Günter Hoch

Institute of Botany, University of Basel, Basel, Switzerland

Author for correspondence:

Tamir Klein

Tel: +41 (0)61 267 3506

Email: tamir.klein@unibas.ch

Received: 26 June 2014

Accepted: 21 July 2014

New Phytologist (2015) **205**: 147–159

doi: 10.1111/nph.12993

Key words: carbon allocation, carbon balance, flux partitioning, phloem transport, soluble sugars, starch, tree compartment.

Summary

- Tree internal carbon (C) fluxes between compound and compartment pools are difficult to measure directly. Here we used a C mass balance approach to decipher these fluxes and provide a full description of tree C allocation dynamics.
- We collected independent measurements of tree C sinks, source and pools in *Pinus halepensis* in a semi-arid forest, and converted all fluxes to g C per tree d⁻¹. Using this data set, a process flowchart was created to describe and quantify the tree C allocation on diurnal to annual time-scales.
- The annual C source of 24.5 kg C per tree yr⁻¹ was balanced by C sinks of 23.5 kg C per tree yr⁻¹, which partitioned into 70%, 17% and 13% between respiration, growth, and litter (plus export to soil), respectively. Large imbalances (up to 57 g C per tree d⁻¹) were observed as C excess during the wet season, and as C deficit during the dry season. Concurrent changes in C reserves (starch) were sufficient to buffer these transient C imbalances.
- The C pool dynamics calculated using the flowchart were in general agreement with the observed pool sizes, providing confidence regarding our estimations of the timing, magnitude, and direction of the internal C fluxes.

Introduction

About 90% of the global biomass of carbon (C) resides in forest trees, and hence their C allocation dynamics are central to global biogeochemistry as well as to their organismal eco-physiology, directly affecting survival and growth (Körner, 2003). Changes in tree C allocation patterns have shown to exert large effects on constituents of the terrestrial C cycle (Luyssaert *et al.*, 2007; Bonan, 2008; Canadell & Raupach, 2008; Reichstein *et al.*, 2013). In trees, the term ‘C allocation’ can describe any of three elements: the flux that transports the C from one locus to another, the target pool in terms of the tree compartment, and the target pool in terms of the C compound. Over the past 35 yr, studies on C allocation typically analyzed one or two of those elements, but rarely all three together (i.e. C fluxes, compartments, and compounds). In some studies, a certain class of C compounds was examined discretely, for example the dynamics of nonstructural carbohydrate (NSC) in stem wood (Barbaroux & Breda, 2002) or branch wood (Schädel *et al.*, 2009). Other studies analyzed both C fluxes and compounds (Vanninen & Mäkelä, 2005; De Swaef *et al.*, 2013), or, alternatively, both C fluxes and compartments (Nygren *et al.*, 1996; Lacoïnte, 2000; Le Roux *et al.*, 2001; Le Goff *et al.*, 2004), or both C compounds and compartments (Hoch *et al.*, 2003; Schädel *et al.*, 2010). To the best of our knowledge, research that considered all three elements of C

allocation was limited to biennials in a glasshouse (Steinlein *et al.*, 1993), studying the effect of resource availability on carbohydrate storage.

To assess C allocation quantitatively, several studies have applied a mass balance approach. An annual C budget for a tree was first calculated, with limited compartment partitioning, by Tranquillini (1979) and by Agren *et al.* (1980). Studies that followed this approach (Le Roux *et al.*, 2001 and references therein) further improved the resolution and increased the complexity of the C budget, with the most detailed flux partitioning presented in Nygren *et al.* (1996). In that study, values of assimilation, respiration, growth, and litter were determined across all tree compartments, with partitioning to foliage, twigs, branches, stem, tap root, and fine roots. However, even in that detailed analysis, many values were not measured directly, but rather modeled or taken from literature data. Other studies calculated C allocation at the forest scale, usually on an annual time-scale (Ryan *et al.*, 1997), also taking advantage of the eddy-covariance method to measure the canopy CO₂ exchange (Waring *et al.*, 1998; Litton *et al.*, 2007; Luyssaert *et al.*, 2007; Rotenberg & Yakir, 2010; Drake *et al.*, 2011). Those studies clearly advanced our understanding of the forest C cycling, but still offered limited information on the partitioning among fluxes and tree compartments (e.g. growth and litter production were often counted together as net primary production; foliage and stem respiration were counted

as above-ground respiration). In addition, in those and all other studies to date, there was no consideration of C allocation to storage in the C budget calculation.

Trees exchange C as CO₂ with the atmosphere, in assimilation (*A*) and respiration (*R*) fluxes, and also release C as litter (*L*) to the forest floor and exudate C to the soil (*E*; export of C to soil). In addition, C is sequestered through growth (*G*). On an annual time-scale, there is a balance between *A* (in a tree-centric view: C source) and all the other fluxes (C sinks):

$$A = R + G + E + L \quad \text{Eqn 1}$$

However, C supply (*A*) and demand (sink activities *R* and *G*, and C loss in *E* and *L*) are not necessarily synchronized at any given time resolution. Trees can buffer C excess by storage (*S*) in C reserves, which can later be consumed (*C*) to buffer C deficit. Therefore, these two fluxes must be considered in a complete C budget, especially for smaller time-scales, that is, at diurnal and monthly time resolution:

$$A = R + G + E + L + S - C \quad \text{Eqn 2}$$

Little is known about the seasonal dynamics of carbon exchange among intrinsic pools, that is, between compartments and between compound-specific pools. These fluxes are difficult to measure in a continuous and nondestructive way. Therefore, previous research has focused on measurements of specific C compounds in phloem and xylem on the one hand (Turgeon & Wolf, 2009; Savage *et al.*, 2013), and modeling of such fluxes based on stem diameter variations on the other hand (Sevanto *et al.*, 2011; De Swaef *et al.*, 2013; Mencuccini *et al.*, 2013). Here, we suggest an alternative approach: combining measurements of C exchange between the tree and its environment and C sequestration (Eqn 1) with the partitioning among internal C pools, structural and nonstructural, should allow the identification of tree intrinsic C transport fluxes.

In this study we took advantage of multi-annual C allocation data compiled from eco-physiological studies of Aleppo pine (*Pinus halepensis*) in Yatir forest, Israel, in 13 yr of continuous research. Here, independent measurements of nearly all tree C sinks, source and pools were collected into a data set, where all fluxes were converted to comparable units (g C per tree d⁻¹). Using this data set, a simple flowchart was created to illustrate the complete, field measurement-based C allocation dynamics across C fluxes, compartments, and compounds. The objectives of this study were: to obtain a balanced C budget in a mature forest tree, by integrating all C fluxes; to test whether the dynamics of starch, that is, the fluxes of storage and consumption, are sufficient to buffer the whole-tree C balance; to test whether the C mass balance approach can reproduce the dynamics of soluble sugars in the tree and its compartments, as periodically measured in different tissues independently; and to define the timing, magnitude, and direction of the intrinsic C fluxes of storage and consumption and of transport between the tree compartments.

Materials and Methods

Data collection and analysis

Tree C pools and fluxes were calculated from independent *in situ* flux- and pool-specific measurements performed between 2000 and 2012 on eight to 28 mature Aleppo pine (*Pinus halepensis* Miller) trees growing in one plot in Yatir forest, Israel (31°20'N, 35°20'E). Aleppo pine is an important forest tree in the Mediterranean region, and the only pine species native to Israel (Quezel, 2000). Temperature and precipitation requirements generally confine its distribution to sub-humid areas of the Mediterranean. With annual precipitation of 285 ± 88 mm, Yatir forest is at the dry edge of the *P. halepensis* distribution. It is a 45-yr-old planted forest, yet all trees have grown under natural conditions, without irrigation or any other treatment. Precipitation is confined to the wet season (December–April) with effectively zero rainfall during the long dry season. As a result of this highly seasonal precipitation distribution, our time-series followed the hydrological year (from 1 October until 30 September) rather than the calendar year. In 2000, an instrumented flux tower was installed in the geographic center of the forest, facilitating multiple eco-physiological studies (Klein *et al.*, 2005; Grünzweig *et al.*, 2007, 2009; Maseyk *et al.*, 2008a,b).

A summary of the source measurements including their respective literature is provided in Table 1. Because of inter-annual variability in flux intensities, fluxes were calculated from multi-annual measurements of 3–10 yr. All C pools and fluxes were transformed into g C per tree and g C per tree d⁻¹, respectively. The diurnal temporal resolution was chosen to better reflect the C allocation dynamics and does not imply a diurnal measurement resolution for the fluxes, which were mostly measured at a weekly, bi-weekly, or monthly temporal resolution. Fluxes and changes in NSC (starch and soluble sugars) pool sizes were calculated down to monthly time resolution. A tree was defined by characteristic diameter at breast height (DBH) of 20 cm and height of 10 m, respectively. These values captured the mean DBH and height of 177 trees measured in the observation plot in 2010 (Jewish National Fund forestry division data). To transform all values into g C, the molar masses of C and CO₂ were applied (12 and 44 g mol⁻¹, respectively), and a molar mass of 30 g mol⁻¹ was used as a general form of carbohydrate (CH₂O). Therefore, measurements of CO₂ fluxes were multiplied by the molar ratio 12/44, and dry biomass values were multiplied by the molar ratio 12/30.

Tree carbon pools

Compartment-specific C pools (Table 2) were calculated for stem, branches and twigs, cones, foliage, and the belowground stem-root transition section, using allometric equations based on the harvest of 28 trees (Grünzweig *et al.*, 2007). C pools in coarse and fine roots were calculated from Maseyk *et al.* (2008a) and Chen *et al.* (2004), respectively. Compound-specific C pools were calculated for starch and soluble sugars in stem, foliage, and roots by multiplying the concentration values (% dry biomass)

Table 1 Tree carbon (C) pools and fluxes and their respective data sources

	Symbol	Data source	Scope and temporal resolution
Pools			
Foliage total C	P_f	Grünzweig <i>et al.</i> (2007)	28 trees; 2003
Stem total C	P_s	Grünzweig <i>et al.</i> (2007)	28 trees; 2003
Root total C	P_r	Grünzweig <i>et al.</i> (2007) Maseyk <i>et al.</i> (2008a)	28 trees; 2003
Foliage NSC	St_f, SS_f	Atzmon <i>et al.</i> (2002)	10 trees; 2000–2001; monthly
Stem NSC	St_s, SS_s	Atzmon <i>et al.</i> (2002) Klein <i>et al.</i> (2014a)	10 trees; 2001, 2012; monthly
Root NSC	St_r, SS_r	Atzmon <i>et al.</i> (2002) Klein <i>et al.</i> (2014a)	10 trees; 2000, 2012; monthly
Fluxes			
Net assimilation	A	Rotenberg & Yakir (2010)	Plot-scale; 2000–2004; daily
Foliage respiration	R_f	Maseyk <i>et al.</i> (2008a)	12 trees; 2002–2004; monthly
Stem respiration	R_s	Maseyk <i>et al.</i> (2008a)	12 trees; 2002–2005; bi-weekly
Root respiration	R_r	Grünzweig <i>et al.</i> (2009)	29 collars; 2000–2006; weekly
Foliage growth	G_f	Grünzweig <i>et al.</i> (2007) Klein <i>et al.</i> (2005)	28 trees; 2003 8 trees; 2000–2004; bi-weekly
Stem growth	G_s	Grünzweig <i>et al.</i> (2007) Klein <i>et al.</i> (2005)	28 trees; 2003 8 trees; 2000–2004; bi-weekly
Root growth	G_r	Grünzweig <i>et al.</i> (2007) Klein <i>et al.</i> (2011)	5 cores; 2007
Foliage litter	L_f	Maseyk <i>et al.</i> (2008b)	25 traps; 2000–2011; bi-weekly
Stem litter	L_s	Maseyk <i>et al.</i> (2008b)	25 traps; 2000–2011; bi-weekly
Cone litter	L_c	Maseyk <i>et al.</i> (2008b)	25 traps; 2000–2011; bi-weekly
Root litter and C export	LE_r	Grünzweig <i>et al.</i> (2007)	5 cores; 2007

NSC, nonstructural carbohydrates.

by the calculated compartment-specific C pools. Measurements of NSC dynamics during 2001 (Atzmon *et al.*, 2002) were used for foliage C pools. In stem and roots, large differences in the NSC distribution among different wood tissues (bark and phloem, sapwood, and heartwood) required a more detailed calculation. NSC dynamics in bark and phloem were obtained from

Table 2 Partitioning of the carbon (C) pools by compartment and compound in a *Pinus halepensis* tree growing in Yatir forest (diameter at breast height (DBH) = 0.2 m; height = 10 m)

Compartment	C content (g C per tree)	Compound	C content (g C per tree)
Stem	32 273		
Branches and twigs	18 610		
Cones	6821		
Total aboveground wood	57 704	St	2020
		SS	3751
		OC	51 934
		St	116
Foliage	5820	SS	146
		OC	5558
Root collar	7723		
Coarse roots	3611		
Fine roots	2367		
		St	548
Total belowground	13 700	SS	754
		OC	12 399
Total tree	77 224		77 224

Compound partitioning is given for October, the beginning of the hydrological year. St, starch; SS, soluble sugars; OC, other, mainly structural, carbon.

Atzmon *et al.* (2002). In sapwood, NSC time-series were measured during 2012 (Klein *et al.*, 2014a), albeit with lower time resolution than in Atzmon *et al.* (2002). Sapwood starch and soluble sugar contents were $41 \pm 4\%$ and $52 \pm 6\%$, respectively, of those of bark and phloem, and hence sapwood NSC dynamics were interpolated using bark and phloem data in months where data were missing. Negligible NSC was assumed for the heartwood tissue of the stem and root collar (Hoch *et al.*, 2003). The partitioning of the stem biomass into its different tissues was estimated by measuring their respective depth at breast height. Bark and phloem depth was determined at 0.7 ± 0.1 cm from 17 trees of DBH = 20.1 ± 0.6 . Sapwood depth was determined at 6.0 cm by sap flow measurement using the heat pulse velocity technique (Cohen *et al.*, 2008). This meant that the stem biomass partitioned into 15.6%, 71.8% and 12.6% bark and phloem, sapwood and heartwood, respectively.

Tree carbon fluxes

C fluxes were calculated from independent *in situ* measurements of (1) C uptake, (2) respiration, (3) growth, and (4) litter production and export to soil. All fluxes were converted into g C per tree d^{-1} and monthly means of diurnal flux rates were integrated into a C allocation data set.

(1) Direct measurements of net carbon assimilation (A) were performed using an infrared gas analyzer (IRGA) chamber gas exchange system, applied extensively during 2000–2004. Yet the large heterogeneity in the light intensity distribution across a tree crown (Welles & Cohen, 1996) introduced a high degree of uncertainty to the upscaling procedure, and called for a more rigorous methodology. Thus, A was downscaled from canopy gross primary productivity (GPP) values calculated from continuous,

in situ eddy-covariance measurements (Rotenberg & Yakir, 2010) and transformed from a land area basis to a single tree basis using the observed stand density (300 trees ha⁻¹). In this semi-arid ecosystem, the understory is very limited, with total biomass reaching 0.3–1 kg DW m⁻² during the wet season, and hence A was well represented by the canopy GPP (Klein *et al.*, 2014b). GPP was calculated from the difference between net ecosystem CO₂ exchange and ecosystem respiration, where the daytime respiration rate was calculated for each day as the mean of the first three half-hours of the preceding night, applying verified, site-specific Q_{10} (short-term temperature sensitivity) values (Grünzweig *et al.*, 2009). The monthly diurnal A values used here are means from downscaled continuous GPP measurement during 2001–2010. To test this approach, GPP-based A values calculated for 2010 were compared with values of A estimated by multiplying sap flow (i.e. the tree transpiration flux, T), which was measured continuously in 10 trees, by water-use efficiency (WUE; i.e. the ratio A/T) derived from time-series of $\delta^{13}\text{C}$ values and daily mean vapor pressure deficit values, as described in Klein *et al.* (2014a), following the studies of Hu *et al.* (2010) and Wang *et al.* (2013). The values obtained by the application of this novel approach showed a high degree of conformity with GPP-based A values both in the total annual value (< 1% discrepancy) and in the daily dynamics ($r^2 = 0.77$ for correlation of 365 daily datapoints). Finally, the monthly mean GPP-based A values were correlated with the aforementioned upscaled needle gas-exchange values, yielding a linear fit with slope of 0.85 and $r^2 = 0.88$.

(2) Nighttime foliage respiration (R_f) and diurnal stem respiration (R_s) were upscaled from IRGA chamber gas exchange measurements performed on 12 trees during 2002–2005 (Maseyk *et al.*, 2008b). CO₂ efflux rates were integrated over the gas exchange period, that is, dark hours and 24 h for R_f and R_s , respectively, and multiplied by the gas exchange surface. For R_f , the surface was the total foliage area, that is, the plot-scale total foliage area calculated by dividing the leaf area index (LAI; 1.5) by the prevailing stand density (300 trees ha⁻¹). For R_s , the surface was the stem surface area, assuming a conical shape, plus the surface area of branches and twigs based on branch length and diameter data from two fallen trees *in situ* (Maseyk *et al.*, 2008a). Root respiration (R_r) was derived from area-based soil respiration (R_{soil}) measurements in 29 collars during 2000–2006 obtained by Grünzweig *et al.* (2009). In that study, the overall annual contribution of heterotrophic respiration to the annual R_{soil} was quantified experimentally as 35%, and hence the annual R_r was calculated as $0.65 \times R_{\text{soil}}$. The monthly dynamics of R_r were constructed using low R_r/R_{soil} ratios in the wet season (0.50 on average) and high R_r/R_{soil} ratios in the dry season (0.75 on average), as also indicated in Grünzweig *et al.* (2009).

(3) C allocation to growth was calculated for the three different tree compartments, namely, foliage, stem, and roots. Foliage growth (G_f) on an annual scale was calculated as 35% of the foliage C pool, because *P. halepensis* in Yatir forest retains needles of four age classes, with a dry biomass fractionation of 0.35, 0.35, 0.20, and 0.10 for 1-, 2-, 3- and 4-yr-old needles, respectively. The calculated annual G_f was similar (95.4%) to the annual foliage litter-fall that was measured directly (item (4) below), as

expected for a steady-state tree foliage biomass. Mean monthly G_f values were then calculated by dividing the annual total according to the mean needle growth curve from eight trees measured in 2000–2004 (Klein *et al.*, 2005). Annual stem growth (G_s) was calculated as 1.95% of DBH, the mean annual DBH increment measured in eight trees, multiplied by the aboveground woody C pools (stem, branches and twigs, and cones). Annual G_s was divided into month-scale rates using the mean stem growth curve (Klein *et al.*, 2005). For comparison, G_s was also calculated from the product of mean basal area increment, obtained from tree-rings, and wood density, and confirmed the values obtained using DBH increments (< 1% discrepancy). Root growth (G_r) was the only C flux that was not measured directly. To estimate it, we multiplied the root C pools (Table 2) by their corresponding root turnovers, estimated from a global root turnover data set (Gill & Jackson, 2000). Considering the annual precipitation and mean air temperature at our site, root turnover was estimated as 0.2 and 0.05 yr⁻¹ for fine roots and coarse roots, respectively. This implied an average fine-root longevity of 5 yr, comparable to values found in *Pinus resinosa* (Aber *et al.*, 1985), but higher than those of other pine species in wet sites (Schoettle & Fahey, 1994). The annual growth of the root collar was calculated by dividing the root collar biomass by its age. The monthly dynamics of G_r were estimated from root biomass increment measurements in *P. halepensis* saplings. A 30-wk dry-down experiment simulating the seasonal drought in Yatir forest showed that G_r was high under wet conditions, peaking at a moderate drought length, and with negligible growth in very dry conditions (Klein *et al.*, 2011). Therefore, G_r was assumed here to be constrained to February–July, and to have a constant growth rate in February–June and a 50% higher growth rate in July.

(4) Loss of C through litter production was quantified using 25 *in situ* litter traps that were monitored on a monthly basis in 2003–2011. Foliage litter (L_f), branch and twig litter (L_s) and cone litter (L_c) were identified and transformed from an area basis to a single tree basis using the observed stand density (300 trees ha⁻¹). Root litter and C export (LE_r) were calculated from an average annual belowground increase in soil C (Grünzweig *et al.*, 2007, 2009) minus the C flux that was retained in the roots (G_r). LE_r lacked information on monthly dynamics, and hence we assumed similar dynamics as for G_r , that is, confinement to February–July with a constant growth rate during February–June and a 50% growth rate in July. Loss of C to herbivores was not quantified but, with very little evidence of herbivory, it was assumed to be negligible.

Integration of the tree carbon pools and fluxes into a carbon allocation flowchart

To integrate the different C fluxes at the whole-tree level, time-series of all C fluxes were fed into two simple, custom-made process flowcharts. The first flowchart showed C allocation patterns at the whole-tree level, with partitioning into C compounds (starch, soluble sugars, and all other C), yielding three C pools connected by five C fluxes (A , R , G , $L + E$ and S/C). The second flowchart showed the same C allocation patterns, with both C

compound and C compartment (foliage, stem, and roots) partitioning, yielding nine pools (3×3) connected by fifteen fluxes (5×3). Diurnal rates of C fluxes, at a monthly time-resolution, and initial pool sizes (Table 2) were calculated from the measurements described in the previous section 'Tree carbon fluxes'. Integrating these data, we were able to calculate diurnal changes in C pool sizes, using a basic algorithm:

$$P_{x(t)} = P_{x(t-dt)} + \sum \text{IF}_{i(t)} - \sum \text{OF}_{i(t)} \quad \text{Eqn 3}$$

where the size of a C pool P_x on a given day (t) was calculated from its size on the preceding day ($t-dt$) plus the sum of all inflows (IF_{*i*}) and minus the sum of all outflows (OF_{*i*}) registered for that day. The monthly means of all fluxes were applied uniformly to all days of the respective month. This algorithm reflects a parsimonious approach, in which the smallest feasible set of assumptions is applied. To test our C balance approach, we calculated changes in the pools of soluble sugars (SS), that is, the balance between all C sources and sinks, and compared them to observed changes in SS as previously reported (Atzmon *et al.*, 2002; Klein *et al.*, 2014).

In the second, compartment-specific flowchart, the root SS pool was tested against the observed changes in root SS while the foliage and stem SS pools did not change. This is because the C transport between the different compartments was calculated using a top-down approach, that is, C flows from one level to the next (from foliage to stem and from stem to roots) only after sinks of the current level have been completed (the 'push theory'; Farrar & Jones, 2000):

$$T_{\text{foliage to stem}} = A + C_f - (R_f + G_f + L_f + S_f); \quad \text{Eqn 4}$$

and:

$$T_{\text{stem to roots}} = T_{\text{foliage to stem}} + C_s - (R_s + G_s + L_s + S_s), \quad \text{Eqn 5}$$

where T is the transport flux and the fluxes A , C , R , G , L and S are assimilation, consumption, respiration, growth, litter production, and storage, respectively.

Standard errors associated with individual C fluxes and pools were taken directly from the source data and represented variations between samples and measurement times, including inter-annual variations among measurements that were taken in a specific month across different years. Errors were downscaled and upscaled together with means. Whole-tree C fluxes and pools were calculated from compartment-specific data, and hence their standard errors were calculated according to error propagation rules (Taylor, 1997); that is, if x and y have independent errors dx and dy , then the error in $z = x + y$ is $dz = (dx^2 + dy^2)^{1/2}$.

Visualization of carbon allocation dynamics

In order to visualize the C allocation dynamics that were calculated from *in situ* measurements and using Eqns (3–5) in the flowcharts, a video file was created for each of the two flowcharts, using Stella simulation tool version 10.0.1 (Isee Systems, San

Diego, CA, USA). Here, this tool was used solely to produce video files, and hence the term 'simulation' does not imply any modeling procedure (although such procedures were available in the software). C pools were defined as stocks and initialized with the measured pool sizes. C fluxes were defined as flows connecting the different stocks, with no further application of any functional relationship; that is, all flows had the basic function 'TIME', described by Eqn 3. The monthly means of all fluxes were applied uniformly to all days of the respective month in a 365-line look-up table that was imported as input to the simulation. Running specifications were defined with 365 d (from 1 October until 30 September) at a 1-d time-step.

Comparative analysis of carbon allocation at the forest scale

Monthly means of tree C fluxes that were calculated from *in situ* measurements were summed at the annual time-scale and compared with respective C fluxes reported in the scientific literature. In many earlier studies, C allocation was studied at the forest scale rather than at the single-tree level (i.e. in g C m^{-2} , rather than g C per tree), and hence we converted our results to a stand area basis, using the observed stand density of 300 trees ha^{-1} . One important advantage of our study site ecosystem was the negligible extent of understory vegetation (Klein *et al.*, 2014b), making this conversion straightforward. For the comparative analysis of C partitioning among the major C sinks (R , G and L) across various forest types, we used the Fluxnet database, as reported in Luyssaert *et al.* (2007). For this purpose, autotrophic respiration, net ecosystem production, and the difference between net primary production and net ecosystem production were identified as our predefined C fluxes R , G and L . For the comparative analysis of the partitioning of the C fluxes R , G and L among the compartments foliage, stem, and roots, we used data from several earlier studies (Ryan *et al.*, 1997; Waring *et al.*, 1998; Law *et al.*, 2001; Litton *et al.*, 2007). In those studies, however, net ecosystem production was not reported, and hence net primary production was used as a proxy for the sum of growth and litter production.

Results

Carbon mass balance at the whole-tree level

Mean diurnal C fluxes ($\text{g C per tree d}^{-1}$) between the tree and its environment were calculated for each month of the hydrological year, from October to September of the following calendar year. Fig. 1 shows the C sinks, in columns, and the C source, assimilation (A), as a curve. Both source and sinks showed an expected bell-shape seasonal pattern with peak intensities in March–April, and significantly lower intensities before and after the wet season (October–November and July–September, respectively). Yet C flux intensity was not entirely synchronized with the timing of precipitation (see the Materials and Methods section), but rather was shifted by 1 month: December fluxes were relatively low, in spite of December being the beginning of the wet season, and

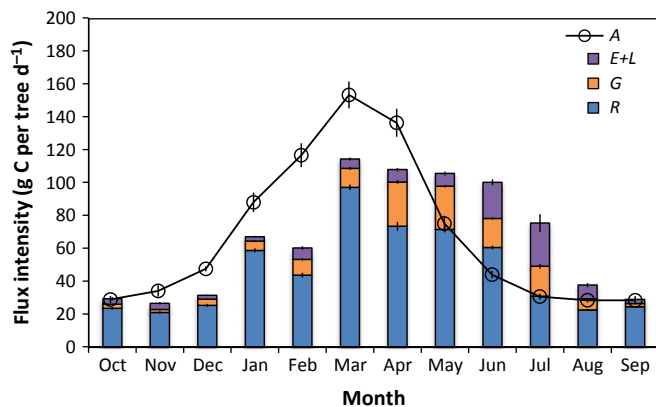


Fig. 1 Monthly dynamics (mean \pm SE) of assimilation (A), respiration (R), growth (G), export to soil (E), and litter production (L) in a mature *Pinus halepensis* tree under semi-arid conditions. Values are based on long-term measurements of the individual fluxes in Yatir forest between 2000 and 2011.

fluxes remained high in May (and June for sinks), beyond the end of the wet season in April. Among C sinks, respiration (R) was the major flux, accounting for 70.3% of the total C sink. Growth (G) and export to soil and litter production ($E + L$) were 17.0% and 12.7% of sinks, respectively. In general, C fluxes peaked during the late wet season (March–April), except for $E + L$, which showed maximum values in June–July.

Integrating the monthly mean diurnal C fluxes over the whole year yielded an annual C source of 24 463 g C per tree yr^{-1} and an annual sum of C sinks of 23 521 g C per tree yr^{-1} . The relatively small discrepancy of 941.8 g C per tree yr^{-1} (3.8%) meant that, on an annual scale, our analysis showed the expected, balanced tree C budget. This annual C turnover of $c.$ 24 kg (excluding C respired by leaves during the daytime) was 30% of the total tree C (77 kg; Table 2), and 12% of the total tree dry biomass (193 kg). A major difference between C source and sinks was in the amplitude of seasonal changes. The intensity ranges of C source and C sinks were 28.7–153.7 and 26.5–114.2 g C per tree d^{-1} , respectively. Source and sink intensities were similar in

September and October, but different in all other months. In February and March, C source was larger than sinks by 39–57 g C per tree d^{-1} , whereas in June and July, C source was smaller than sinks by 44–56 g C per tree d^{-1} . The large monthly scale C imbalance meant that the tree had to buffer the large gaps between C source and sinks, and suggested an important role for C reserves.

Integration of compound-specific pools into a whole-tree carbon allocation flowchart

The mass balance between C source and C sinks (Fig. 1) is schematically described in Fig. 2(a). Such a C balance provides no information on C partitioning between intrinsic C pools and their dynamics, that is, C allocation fluxes, and hence the tree C pool is essentially a black box. To examine this, we introduced the internal C pools of soluble sugars (SS), starch (St) and new, current-year C other than soluble sugars or starch (NC), and the internal fluxes of storage (i.e. St formation; S) and consumption (i.e. St degradation; C). Compound-specific pools were then integrated into a whole-tree C allocation flowchart, schematically described in Fig. 2b. The assimilated C joins the tree SS pool, where it may change its form and flow in one of three fluxes: respiration as CO_2 (R); synthesis into another C compound (e.g. cellulose, lignin, or amino acids) and integration into tree tissues as part of growth (G); or synthesis into St as part of storage (S). The S/C flux is unique in the sense that it is assumed to be the only bi-directional flux: carbon may flow back from the St pool into the SS pool following starch hydrolysis. C losses to the environment also include litter production (L) and export to soil (E).

To describe the tree C allocation dynamics and test the hypothesis that C reserves can buffer short-term imbalances between C source and sinks, a simple whole-tree C allocation flowchart was constructed. In this flowchart, C fluxes and pools followed the detailed C balance scheme (Fig. 2b), with flux intensities (Fig. 1) and starch dynamics as input. To initialize the calculation of specific pool sizes, estimates of compound-specific C pool sizes were used (Table 2). The flowchart output was the changes in the three compound-specific C pools that were

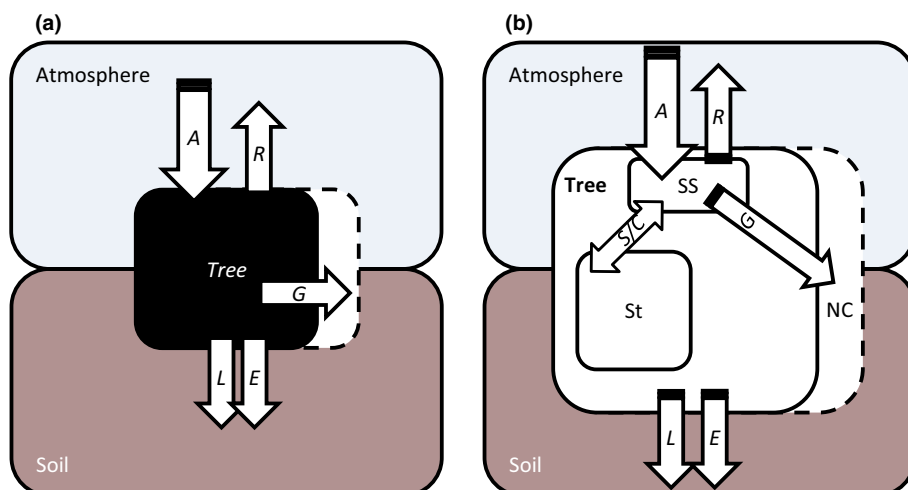


Fig. 2 Carbon (C) fluxes in a tree depicted by a 'black box' flow diagram (a) and with partitioning among internal C pools (b). Fluxes are: A , assimilation; R , respiration; G , growth; E , export to soil; L , litter production; and S/C , storage/consumption of C reserves. Pools are: SS, soluble sugars; St, starch; and NC, new, current-year C.

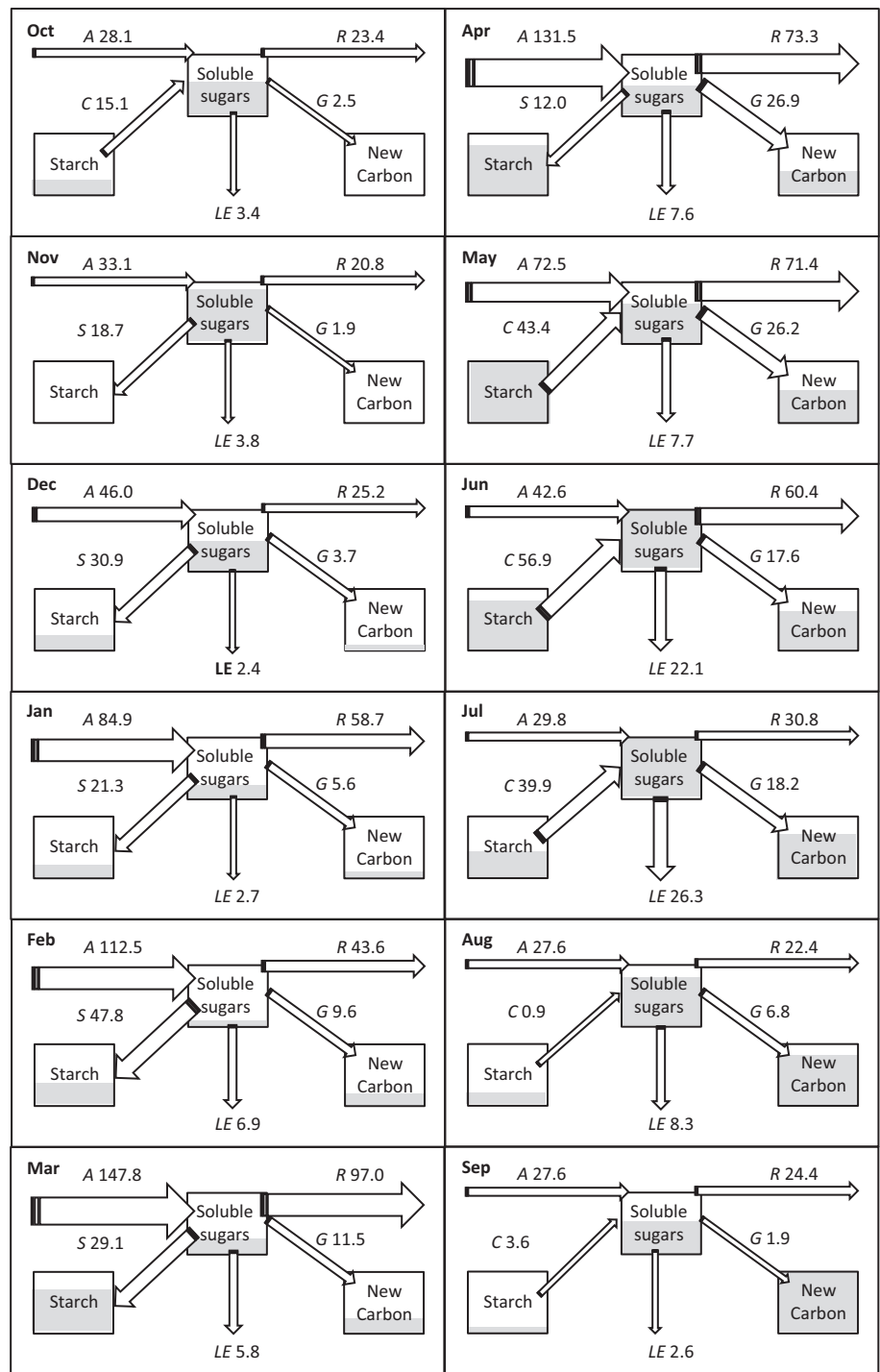


Fig. 3 Whole-tree carbon (C) allocation dynamics in 12 months based on C flux intensities and starch dynamics in a mature *Pinus halepensis* tree. The widths of the arrows are proportional to flux intensities (g C per tree d⁻¹), and fluctuations in the size of each C pool noted by its relative saturation, between its annual minimum and maximum values. Fluxes are: A, assimilation; R, respiration; G, growth; LE, litter production and export to soil; S, storage; and C, consumption.

calculated in diurnal steps (Supporting Information Video S1). Fig. 3 shows monthly C allocation dynamics, with fluctuations in the size of each C pool noted by its relative saturation, between its annual minimum and maximum values. The St pool increased mostly during December–March (large inflows) and decreased during May–July (large outflows). The NC pool increased gradually throughout the year (but less so during September–November), with most of the increase during April–July. Within the flowchart, the C balance between A, R, G, LE and S/C was

calculated as changes in the SS pool, which decreased between November and February and increased between March and June. Comparing these calculated SS levels (Fig. 3) to SS measurements showed generally similar behavior, with discrepancies in the magnitude of the seasonal dynamics (Fig. 4). The calculation yielded smaller fluctuations in SS than observed, yet captured the general dynamics and the SS value at the end of the year. A correlation based on 11 data-points (the October value was not calculated but rather used to initialize the flowchart) produced the linear fit:

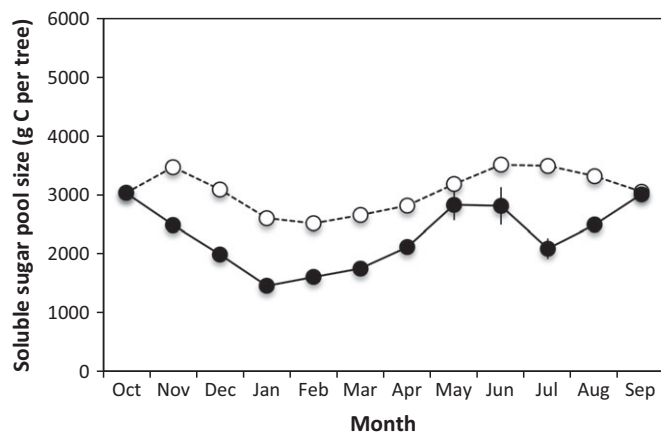


Fig. 4 Calculated (open circles) versus observed (closed circles) changes in soluble sugar content in a mature *Pinus halepensis* tree under semi-arid conditions (mean \pm SE). A correlation based on 11 data-points (the October value was measured) produced the linear fit: calculated SS = $0.49 \times$ measured SS + 1959 ($r^2 = 0.48$; $P = 0.016$).

calculated SS = $0.49 \times$ measured SS + 1959 ($r^2 = 0.48$; $P = 0.016$).

Compartment-specific carbon allocation flowchart

Whole-tree flux intensities (Fig. 1) were calculated by integrating measurements of fluxes at three compartments, that is foliage, stem, and roots, indicated by the subscripts f, s and r, respectively (Table 1). To better exploit the data that were collected, C sinks were partitioned into compartment-specific sinks (Fig. 5). Foliage dominated EL ($L_f/EL = 0.65$), and, to a lesser extent, G ($G_f/G = 0.51$) as a result of high fluxes in the late spring and summer months. R was dominated by roots ($R_r/R = 0.61$), which respired at rates of 40–75 g C per tree d^{-1} in March–June. As St content dynamics were also available for all three compartments, the C allocation flowchart (Fig. 3) was expanded to include both compound- and compartment-specific fluxes (Fig. 6). In this flowchart, compound-specific C pools followed the description in the whole-tree flowchart (from left to right: St, SS and NC), while compartment-specific C pools were laid out intuitively, from foliage at the top, through stem in the middle to roots at the bottom. Four additional internal fluxes were constructed to allow C transport between leaves and stem and between stem and roots. Transport flux intensities were calculated using Eqns 4 and 5 and hence changes in foliage and stem SS pools could not be captured. The flowchart output was the changes in the nine compound- and compartment-specific C pools that were calculated in diurnal steps (Video S2). Mean diurnal C allocation dynamics during October, January, April, and July showed major seasonal shifts in all C pools (Fig. 6). During October, all C fluxes were relatively small and St pools low. In January, most C fluxes were higher, especially above ground. All St pools increased, and NC increased in the stem. The increased C transport to roots was allocated mostly to root respiration. During April, the high C influx through an increased assimilation rate was distributed to all C pools above and below ground, saturating all St pools

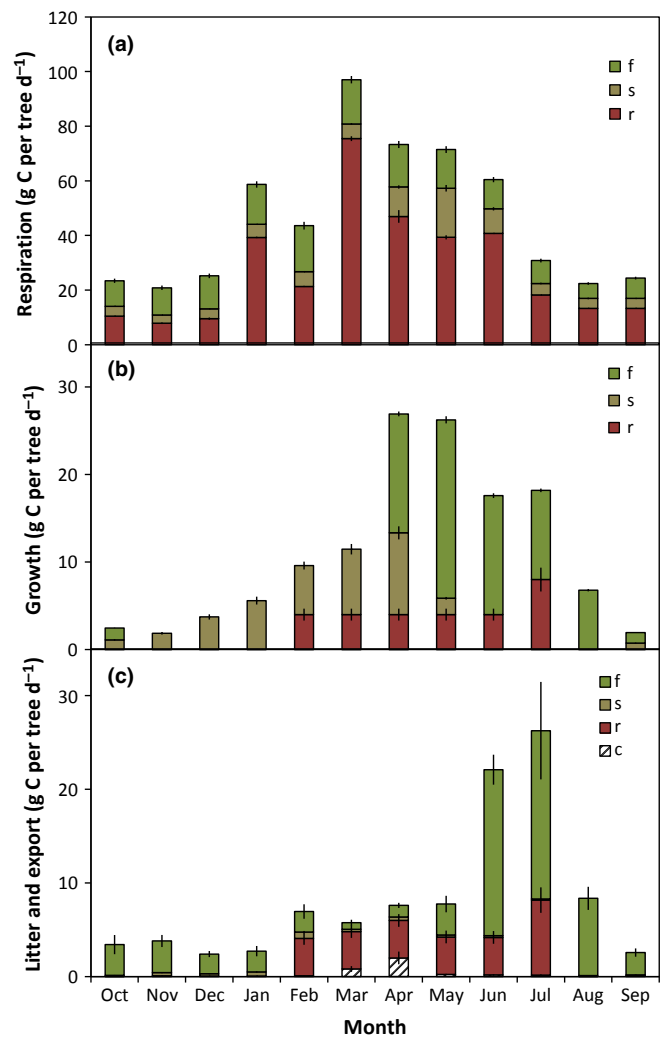


Fig. 5 Partitioning of monthly carbon sinks (respiration (a), growth (b), and litter and export (c); all are mean \pm SE) by compartment (f, foliage; s, stem; r, roots; and c, cones) in a mature *Pinus halepensis* tree under semi-arid conditions. Values are based on long-term measurements of individual fluxes in Yatir forest between 2000 and 2011.

and increasing stem and root NC pools. In July, lower St pools indicated the ongoing consumption of St (note the change in arrow direction from St to SS pools), in parallel with continued growth in foliage and roots. Calculated changes in the SS_r pool were compared with the measured values (Fig. 7). The C balance-based calculation overestimated SS_r during November–December and May–August by up to 83% in June, and underestimated SS_r by up to 62% during most of the wet season. Yet the general SS_r dynamics and final value were captured with relatively good agreement. A correlation produced the linear fit: calculated $SS_r = 2.25 \times$ measured $SS_r - 550$ ($r^2 = 0.68$; $P = 0.002$). Fig. 8 shows the intensity of C transport between the compartments, which generally followed the increase in C allocation in the wet season, and the subsequent decrease in the dry season. In July and August, C fluxes had negative values, indicating relocation fluxes, that is, from stem to foliage, and from roots to stem, respectively.

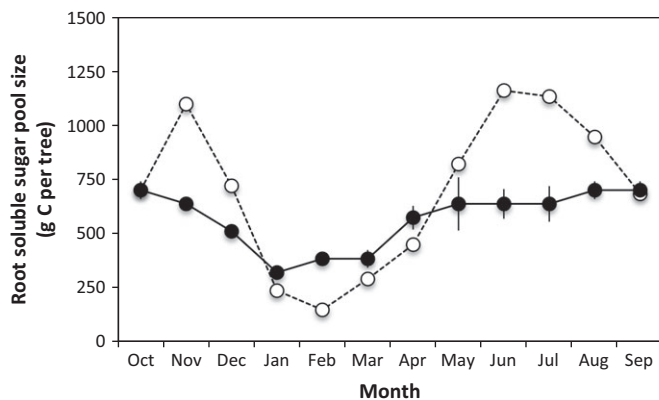


Fig. 7 Calculated (open circles) versus observed (closed circles) changes in root soluble sugar content (SS_r) in a mature *Pinus halepensis* tree under semi-arid conditions (mean \pm SE). A correlation based on 11 data-points (the October value was measured) produced the linear fit: calculated $SS_r = 2.25 \times$ measured $SS_r - 550$ ($r^2 = 0.68$; $P = 0.002$).

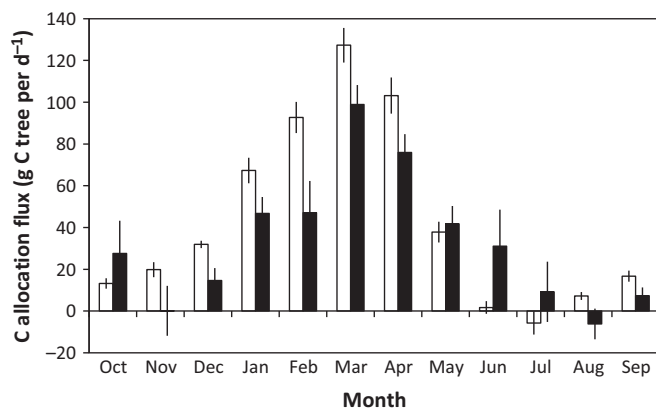


Fig. 8 Carbon (C) allocation fluxes (mean \pm SE) between compartments in a mature *Pinus halepensis* tree under semi-arid conditions. Open bars, foliage to stem; closed bars, stem to roots. Negative C fluxes, in July and August, indicate relocation fluxes, that is, from stem to foliage, and from roots to stem, respectively.

ratio $(G + D)/A$, also termed carbon use efficiency, has long been reported to be $c. 0.40$, indicating the 'carbon cost' of respiration (Ryan *et al.*, 1997). To what extent are these C partitioning patterns different from the patterns of forest trees in other sites? One indication comes from information on CO_2 fluxes over forest canopies, which include additional components (e.g. CO_2 exchange of the understory and heterotrophic respiration from soil), but for which there are more available than for tree-scale C balance. Measurements from the Yatir forest flux tower, over the trees that were included in this study, show that the mean annual C uptake and ecosystem respiration fluxes are 820 and 600 $g C m^{-2} y^{-1}$, respectively (Rotenberg & Yakir, 2010). This yields an R/A ratio of 0.73, slightly higher than the tree-scale value of 0.70 reported here, which is expected considering the contribution of soil respiration to the ecosystem C exchange. A meta-analysis of C flux data from 12 European pine forests and from the entire Fluxnet network (Luyssaert *et al.*, 2007) yields an R/A ratio of 0.83, indicating an even larger partitioning to

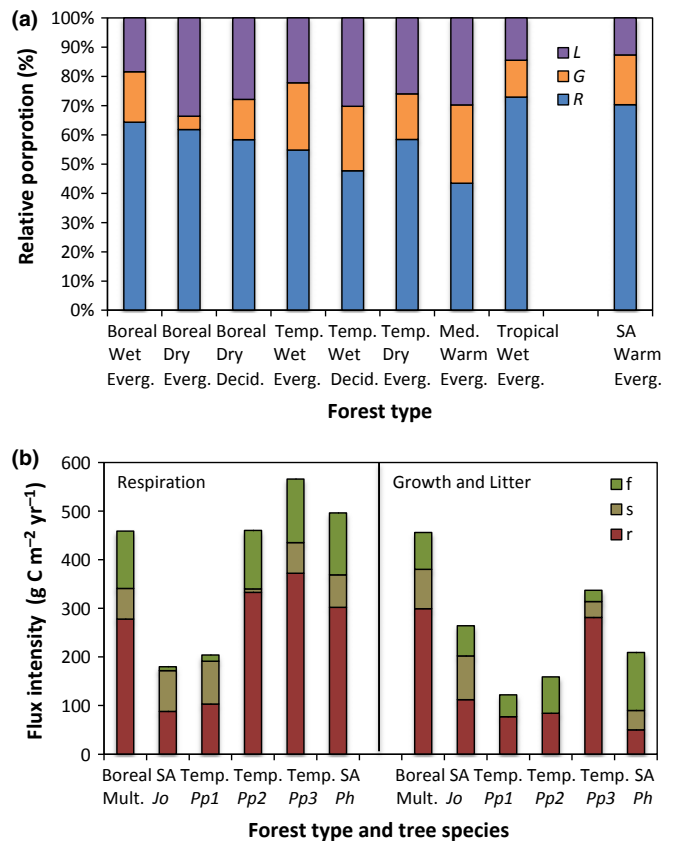


Fig. 9 Partitioning of the major tree carbon (C) sinks on an annual time-scale and on a forest area basis in this study (right-end bars in (a); SA) and in earlier studies of C allocation at the forest scale. (a) The partitioning among major C sinks (L , litter production; G , growth; and R , respiration) across various forest types from the Fluxnet database ($n = 18\text{--}96$ sites per type; Luyssaert *et al.*, 2007). (b) The partitioning of respiration and the sum of growth and litter production among the compartments foliage (f), stem (s), and roots (r) in earlier studies (from left: Ryan *et al.*, 1997, multiple species; Waring, *et al.*, 1998, Jo, Pp1; Law *et al.*, 2001, Pp2; Litton *et al.*, 2007, Pp3) and in this study. Temp., temperate; Med., Mediterranean; SA, semi-arid (this study); Everg., evergreen; Decid., deciduous; Mult., multiple species; Jo, *Juniperus occidentalis*; Pp, *Pinus ponderosa*; Ph, *Pinus halepensis*.

respiration. Considering most forest types around the globe, the relative portions of C allocated to R , G and L are 0.43–0.73, 0.05–0.27 and 0.13–0.34, respectively (Fig. 9a). This comparative analysis also shows that the partitioning among C sinks is not directly related to biome, water availability (wet/dry) or foliage cover (evergreen/deciduous). Evidently, our results are most similar to those for the contrasting tropical wet forest and the boreal wet evergreen forest, and least similar to those for the Mediterranean forest (Fig. 9a). It is possible that the high C partitioning to G and L in the Mediterranean forest is related to a high abundance of summer-deciduous broadleaf species, which are absent in our semi-arid ecosystem. Nevertheless, Waring *et al.* (1998) found the highest tree R/A ratio (0.60) among 12 forest sites in a semi-arid forest, and Litton *et al.* (2007) found an increase in R/A ratio with decreasing A .

Previous studies of the C balance at the tree scale have shown a different flux partitioning than here, with growth estimated as

Table 3 Flux and compartment partitioning (g C per tree yr⁻¹) of the tree carbon (C) balance in this study and in previous studies

	Symbol	Agren <i>et al.</i> (1980)	Nygren <i>et al.</i> (1996)	Le Goff <i>et al.</i> (2004)	This study
Forest biome		Boreal	Tropical	Temperate	Semi-arid
Tree species		<i>Pinus sylvestris</i>	<i>Erythrina poeppigiana</i>	<i>Fraxinus excelsior</i>	<i>Pinus halepensis</i>
Tree age (yr)		14	2	25	35–45
Tree height (m)		2.8	3.7	17.1	10.0
Tree DBH (cm)		NA	NA	18.2	20.0
Flux					
Net assimilation	A	1723	13 666	20 590	24 463
Foliage respiration	R_f	NA	2930	3470	4222
Stem respiration	R_s	64	NA	NA	2246
Root respiration	R_r	109	2076	4548	10 074
$R/(R + G + LE)$		10%	36%	32%	70%
Foliage growth	G_f	286	2044	3060	2037
Stem growth	G_s	277	4302	11 110	1120
Root growth	G_r	960	1280	2500	834
$G/(R + G + LE)$		90%	55%	68%	17%
Foliage litter	L_f	NA	1128	NA	1943
Stem litter	L_s	NA	NA	NA	92
Reproduction litter	L_c	NA	NA	NA	114
Root litter and C export	LE_r	NA	NA	NA	840
$LE/(R + G + LE)$		NA	8%	NA	13%

DBH, diameter at breast height; NA, not available.

the major flux (Table 3). Unfortunately, two of these three earlier studies were performed on young trees and saplings (Agren *et al.*, 1980; Nygren *et al.*, 1996, respectively), which can have substantial differences in C metabolism from mature trees. Le Goff *et al.* (2004) analyzed the C balance of 25-yr-old *Fraxinus excelsior*, but did not quantify any litter and export fluxes. This was in spite of the fact that A was smaller by 14% than the sum of calculated C sinks in that study. All three studies disregarded important compartment-specific fluxes, such as stem and foliage respiration. Finally, the estimation of many of the C fluxes in those earlier studies was rather crude, and often relied on simulated data or literature data used under some assumptions. Therefore, it is possible that the C flux partitioning in previous studies overestimated growth as the major C flux in a tree, supporting the biased view of a growth-dominated C balance. Our results, together with forest flux measurements applying advanced micrometeorological techniques such as eddy covariance (Bonan, 2008; Reichstein *et al.*, 2013), call into question the validity of this view.

The partitioning of C fluxes into the tree's compartments (Fig. 5) can be also compared with the results of earlier studies (Table 3), with some degree of uncertainty. The annual C uptake calculated for 25-yr-old *F. excelsior* (Le Goff *et al.*, 2004) was relatively close to the value estimated here. Results from that study and from Agren *et al.* (1980) were also in agreement with the major role of roots in the tree's respiration flux. Yet our observation of the foliage as a major sink for growth differed from the other studies, which suggested that growth was dominated by the stem or the roots. Again, the comparison to forest-scale studies yielded better agreement with our results (Fig. 9b). Roots dominate the respiration flux and, to a lesser extent, the sum of growth and litter. Focusing on growth, the relative proportion of C allocated to foliage is *c.* 0.70 (Brüggemann *et al.*, 2011; and

references therein), higher than our ratio of 0.51. C allocated to stem growth is always smaller than that allocated to foliage or roots, and the only facultative G flux (Litton *et al.*, 2007).

Intrinsic carbon fluxes and the role of starch as a carbon reserve

Our analysis showed large imbalances between C source and sinks (up to 57 g C per tree d⁻¹), which were observed as C excess during the wet season, and as C deficit during the dry season (Fig. 1). Starch dynamics were sufficient to buffer these gaps, as C excess was stored in this pool during November–April, and consumed during May–October. Fig. 3 shows that in June and July starch consumption became the major C source for the tree, supplying C at rates of 57 and 40 g C per tree d⁻¹, respectively, compared with the lower rates of assimilation (43 and 30 g C per tree d⁻¹, respectively). Yet at the compartment level, it is possible that the 'local' starch pool was insufficient to match C demands. Evidently, our three-compartment C flowchart demonstrated that C allocation between discrete compartments could be bi-directional, with the existence of two relocation flows: C transport from roots to the stem, and from the stem to the leaves (Fig. 6). These flows were relatively minor in size (5.7 g C per tree d⁻¹ and 6.2 g C per tree d⁻¹, respectively), within the magnitude of the calculated error, and restricted to the peak drought months of July–August. The potential C relocation to the leaves in July correlated with a minimum in the foliage starch pool, while the stem starch pool was also close to its lowest level. The potential relocation from roots to the stem in August did not correlate with such a local minimum in either stem or roots. In both cases, and at all times, all three compartments had some amount of starch. The first relocation (from stem to foliage) suggests some low threshold level at which local starch hydrolysis

stops and C must be imported into leaves, in agreement with Hoch (2005). The second relocation (from roots to stem) might suggest that C transport within the tree is governed by sink activities rather than supply level, as discussed in earlier studies (Farrar & Jones, 2000). It would be interesting to determine to what extent these relocation flows can change (e.g. increase under environmental stress) and whether such C management changes offer any advantage to tree fitness and drought resistance.

The C pool dynamics estimates yielded by our simple flowchart were in partial agreement with the observed pool sizes (Figs 4, 7). However, discrepancies still existed, and could be related to one or more of the following reasons: (1) uncertainties related to some of the C fluxes, especially to belowground fluxes (root growth, root respiration, and C export to soil), which involved multiple assumptions and indirect estimations; (2) uncertainties related to changes in the NSC pools, which were derived from measurements over 2 yr only; (3) inter-annual differences which could affect the flux intensity estimation, considering the unequal span of data sources (Table 1; for example, stem respiration was measured in 2002–2005, a set of wet years, whereas litter production was measured in 2000–2011, integrating some drier years); (4) the existence of other mobile C pools, such as lipids or other nonstructural compounds such as resin, which are quite abundant in pine tissues; (5) a possible reserve function of some structural C compounds, such as hemicelluloses (Hoch, 2007; Schädel *et al.*, 2009, 2010). Considering the high number of uncertainties, any concrete statement about the source of the discrepancy would be highly speculative.

Combining stem diameter variation measurements and complex mechanistic modeling, De Swaef *et al.* (2013) were able to predict dynamics in phloem sugar loading in tomato (*Solanum lycopersicum*) grown in the glasshouse. Our results suggest that, using direct measurements of C fluxes, this approach can potentially be extended to mature forest trees in the field. It might thus contribute to quantitative assessment of phloem C transport dynamics, which are currently not well understood and very difficult to measure in mature trees (Windt *et al.*, 2006; Mencuccini *et al.*, 2013). Another promising approach uses C isotope fractionation to follow C allocation dynamics in trees (reviewed in Brüggemann *et al.*, 2011). Integration of such data into the C allocation flowchart presented here is among our future research assignments. This is of key importance considering the need to improve our understanding of tree C management and its sensitivity to environmental perturbations such as CO₂ increase and drought stress.

Acknowledgements

The authors thank Jose Grünzweig of the Hebrew University of Jerusalem and Dan Yakir of the Weizmann Institute of Science for their useful discussions at earlier stages of this project. Christophe Randin of the University of Basel is acknowledged for assistance with simulations using Stella. Three anonymous referees are gratefully acknowledged for their useful comments, which were critical in helping to improve this paper. T.K. receives funding from Plant Fellows, an international Post Doc Fellowship

Program in Plant Sciences of the Zürich-Basel Plant Science Center (PSC). The research was co-funded by the EU FP7 Marie Curie actions and the Swiss National Fund project FORCARB (31003A_14753/1) allocated to the Basel Plant Ecology group headed by Christian Körner. G.H. received funding from the European Research Council (ERC) grant no. 2333; project TRE-ELIM to Christian Körner) during parts of the work for this study.

References

- Aber JD, Melillo JM, Nadelhoffer KJ, McCaughery CA, Pastor J. 1985. Fine root turnover in forest ecosystems in relation to quality and form of nitrogen availability: a comparison of two methods. *Oecologia* **66**: 317–321.
- Agren GI, Axelsson B, Flower-Ellis JGK, Linder S, Persson H, Stall H, Troeng E. 1980. Annual budget for a young Scots pine. *Ecological Bulletins* **32**: 307–313.
- Atzmon N, Schiller G, Riov Y. 2002. Survey of seasonal carbohydrate level fluctuations as a basis to understand development and growth of forest trees in Israel. KKL-JNF Report #90-3-085-02.
- Barbaroux C, Breda N. 2002. Contrasting distribution and seasonal dynamics of carbohydrate reserves in stem wood of adult ring-porous sessile oak and diffuse-porous beech trees. *Tree Physiology* **22**: 1201–1210.
- Bonan GB. 2008. Forests and climate change: forcings, feedbacks, and the climate benefits of forests. *Science* **320**: 1444–1449.
- Brüggemann N, Gessler A, Kayler Z, Keel SG, Badeck F, Barthel M, Boeckx P, Buchmann N, Brugnoli E, Esperschütz J *et al.* 2011. Carbon allocation and carbon isotope fluxes in the plant-soil-atmosphere continuum: a review. *Biogeosciences* **8**: 3457–3489.
- Canadell JG, Raupach MR. 2008. Managing forests for climate change mitigation. *Science* **320**: 1456–1457.
- Chen WJ, Zhang QF, Cihlar J, Bauhus J, Price DT. 2004. Estimating fine-root biomass and production of boreal and cool temperate forests using aboveground measurements: a new approach. *Plant and Soil* **265**: 31–46.
- Cohen Y, Cohen S, Cantuarias-Aviles T, Schiller G. 2008. Variations in the radial gradient of sap velocity in trunks of forest and fruit trees. *Plant and Soil* **305**: 49–59.
- De Swaef T, Driever SM, van Meulebroek L, Vanhaecke L, Marcelis LFM, Steppe K. 2013. Understanding the effect of carbon status on stem diameter variations. *Annals of Botany* **111**: 31–46.
- Drake JE, Davis SC, Raetz LM, DeLucia EH. 2011. Mechanisms of age-related changes in forest production: the influence of physiological and successional changes. *Global Change Biology* **17**: 1522–1535.
- Farrar JF, Jones DL. 2000. The control of carbon acquisition by roots. *New Phytologist* **147**: 43–53.
- Gill RA, Jackson RB. 2000. Global patterns of root turnover for terrestrial ecosystems. *New Phytologist* **147**: 13–31.
- Grünzweig JM, Gelfand I, Yakir D. 2007. Biogeochemical factors contributing to enhanced carbon storage following afforestation of a semi-arid shrubland. *Biogeosciences* **4**: 891–904.
- Grünzweig JM, Hemming D, Maseyk K, Lin T, Rotenberg E, Raz-Yaseef N, Falloon PD, Yakir D. 2009. Water limitation to soil CO₂ efflux in a pine forest at the semiarid “timberline”. *Journal of Geophysical Research* **114**: G03008.
- Hoch G. 2005. Fruit-bearing branchlets are carbon autonomous in mature broad-leaved temperate forest trees. *Plant, Cell & Environment* **28**: 651–659.
- Hoch G. 2007. Cell wall hemicelluloses as mobile carbon stores in non-reproductive plant tissues. *Functional Ecology* **21**: 823–834.
- Hoch G, Richter A, Körner C. 2003. Non-structural carbon compounds in temperate forest trees. *Plant, Cell & Environment* **26**: 1067–1081.
- Hu J, Moore DJP, Riveros-Iregui DA, Burns SP, Monson RK. 2010. Modeling whole-tree carbon assimilation rate using observed transpiration rates and needle sugar carbon isotope ratios. *New Phytologist* **185**: 1000–1015.

- Klein T, Cohen S, Yakir D. 2011. Hydraulic adjustments underlying drought resistance of *Pinus halepensis*. *Tree Physiology* 31: 637–648.
- Klein T, Hemming D, Lin T, Grunzweig JM, Maseyk K, Rotenberg E, Yakir D. 2005. Association between tree-ring and needle delta C-13 and leaf gas exchange in *Pinus halepensis* under semi-arid conditions. *Oecologia* 144: 45–54.
- Klein T, Hoch G, Yakir D, Körner C. 2014a. Drought stress, growth, and nonstructural carbohydrate dynamics of pine trees in a semi-arid forest. *Tree Physiology*, in press.
- Klein T, Rotenberg E, Cohen-Hilaleh E, Raz-Yaseef N, Tatarinov F, Ogée J, Cohen S, Yakir D. 2014b. Quantifying transpirable soil water and its relations to tree water use dynamics in a water-limited pine forest. *Ecophysiology* 7: 409–419.
- Körner C. 2003. Carbon limitation in trees. *Journal of Ecology* 91: 4–17.
- Lacointe A. 2000. Carbon allocation among tree organs: a review of basic processes and representation in functional-structural tree models. *Annals of Forest Science* 57: 521–533.
- Law BE, Thornton PE, Irvine J, Anthoni PM, Van Tuyl S. 2001. Carbon storage and fluxes in ponderosa pine forests at different developmental stages. *Global Change Biology* 7: 755–777.
- Le Goff N, Granier A, Ottorini J-M, Pfeiffer M. 2004. Biomass increment and carbon balance of ash (*Fraxinus excelsior*) trees in an experimental stand in northern France. *Annals of Forest Science* 61: 1–12.
- Le Roux X, Lacointe A, Escobar-Gutierrez A, Le Dizes S. 2001. Carbon-based models of individual tree growth: a critical appraisal. *Annals of Forest Science* 58: 469–506.
- Litton CM, Raich JW, Ryan MG. 2007. Carbon allocation in forest ecosystems. *Global Change Biology* 13: 2089–2109.
- Luyssaert S, Inglis I, Jung M, Richardson D, Reichstein M, Papale D, Piao SL, Schulze E-D, Wingate L, Matteucci G *et al.* 2007. CO₂ balance of a boreal, temperate, and tropical forests derived from a global database. *Global Change Biology* 13: 2509–2537.
- Maseyk KS, Grunzweig JM, Rotenberg E, Yakir D. 2008a. Respiration acclimation contributes to high carbon-use efficiency in seasonally dry pine forest. *Global Change Biology* 14: 1–15.
- Maseyk KS, Lin T, Rotenberg E, Grunzweig JM, Schwartz A, Yakir D. 2008b. Physiology–phenology interactions in a productive semi-arid pine forest. *New Phytologist* 178: 603–616.
- Mencuccini M, Hölttä T, Sevanto S, Nikinmaa E. 2013. Concurrent measurements of change in the bark and xylem diameters of trees reveal a phloem-generated turgor signal. *New Phytologist* 198: 1143–1154.
- Muller B, Pantin F, Genard M, Turc O, Freixes S, Piques M, Gibon Y. 2011. Water deficits uncouple growth from photosynthesis, increase C content, and modify the relationships between C and growth in sink organs. *Journal of Experimental Botany* 62: 1715–1729.
- Nygren P, Kiema P, Rebottaro S. 1996. Canopy development, CO₂ exchange and carbon balance of a modeled agroforestry tree. *Tree Physiology* 16: 733–745.
- Quezel P. 2000. Taxonomy and biogeography of Mediterranean pines (*Pinus halepensis* and *P. brutia*). In: Ne'eman G, Trabaud L, eds. *Ecology, biogeography and management of Pinus halepensis and P. brutia forest ecosystems in the Mediterranean basin*. Leiden, the Netherlands: Backhuys Publishers, 1–12.
- Reichstein M, Bahn M, Ciais P, Frank D, Mahecha MD, Senevirante SI, Zscheischlwe J, Beer C, Buchmann N, Frank DC. 2013. Climate extremes and the carbon cycle. *Nature* 500: 287–295.
- Rotenberg E, Yakir D. 2010. Contribution of semi-arid forests to the climate system. *Science* 327: 451–454.
- Ryan MG, Lavigne MB, Gower ST. 1997. Annual carbon cost of autotrophic respiration in boreal forest ecosystems in relation to species and climate. *Journal of Geophysical Research* 102: 28871–28884.
- Savage JA, Zwieniecki MA, Holbrook NM. 2013. Phloem transport velocity varies over time and among vascular bundles during early cucumber seedling development. *Plant Physiology* 163: 1409–1418.
- Schädel C, Richter A, Bloechl A, Hoch G. 2009. Short-term dynamics of nonstructural carbohydrates and hemicellulose in young branches of temperate forest trees during bud break. *Tree Physiology* 29: 901–911.
- Schädel C, Richter A, Bloechl A, Hoch G. 2010. Hemicellulose concentration and composition in plant cell walls under extreme carbon source-sink imbalances. *Physiologia Plantarum* 139: 241–255.
- Schoettle AW, Fahey TJ. 1994. Foliage and fine root longevity of pines. *Ecological Bulletins* 43: 136–153.
- Sevanto S, Hölttä T, Holbrook M. 2011. Effects of the hydraulic coupling between xylem and phloem on diurnal phloem diameter variation. *Plant, Cell & Environment* 34: 690–703.
- Steinlein T, Heilmeyer H, Schulze E-D. 1993. Nitrogen and carbohydrate storage in biennials originating from habitats of different resource availability. *Oecologia* 93: 374–382.
- Taylor JR. 1997. *An introduction to error analysis*. California, CA, USA: University Science Books.
- Tranquillini W. 1979. *Physiological ecology of the alpine timberline*. *Ecological Studies* 31. Berlin, Heidelberg, Germany, New York, NY, USA: Springer-Verlag.
- Turgeon R, Wolf S. 2009. Phloem transport: cellular pathways and molecular trafficking. *Annual Review of Plant Biology* 60: 207–221.
- Vanninen P, Mäkelä A. 2005. Carbon budget for Scots pine trees: effects of size, competition and site fertility on growth allocation and production. *Tree Physiology* 25: 17–30.
- Wang H, Zhao P, Zou LL, McCarthy HR, Zeng XP, Ni GY, Rao XQ. 2013. CO₂ uptake of a mature *Acacia mangium* plantation estimated from sap flow measurements and stable carbon isotope discrimination. *Biogeosciences Discussions* 10: 11583–11625.
- Waring RH, Landsberg JJ, Williams M. 1998. Net primary production of forests: a constant fraction of gross primary production? *Tree Physiology* 18: 129–134.
- Welles JM, Cohen S. 1996. Canopy structure measurement by gap fraction analysis using commercial instrumentation. *Journal of Experimental Botany* 47: 1335–1342.
- Windt CW, Vergeldt FJ, De Jager PA, Van As H. 2006. MRI of long-distance water transport: a comparison of the phloem and xylem flow characteristics and dynamics in poplar, castor bean and tobacco. *Plant, Cell & Environment* 29: 1715–1729.

Supporting Information

Additional supporting information may be found in the online version of this article.

Video S1 Diurnal changes over the year in the three compound-specific carbon pools in a mature *Pinus halepensis* tree under semi-arid conditions, as simulated using measured carbon fluxes.

Video S2 Diurnal changes over the year in the nine compound- and compartment-specific carbon pools in a mature *Pinus halepensis* tree under semi-arid conditions, as simulated using measured carbon fluxes.

Please note: Wiley Blackwell are not responsible for the content or functionality of any supporting information supplied by the authors. Any queries (other than missing material) should be directed to the *New Phytologist* Central Office.